The International Journal of Advanced Manufacturing Technology (2023) 128:3215–3232
https://doi.org/10.1007/s00170-023-12143-0

ORIGINAL ARTICLE

Effective feed rate control to maintain constant feed per tooth along toolpaths for milling complex–shaped parts

Petr Vavruska[1] · Filip Bartos[1] · Matej Pesice[1]

Received: 20 March 2023 / Accepted: 10 August 2023 / Published online: 17 August 2023

Abstract
Constantly increasing demands for accuracy, surface quality, and higher production productivity associated with machining time reduction, all of which are to be achieved together with a cost-savings demand, create room for production optimization in complex part machining. This is especially true for difficult-to-machine materials, where great emphasis is placed on maintaining the technological conditions during machining, as the optimum value adjustment range is very narrow. When milling complex–shaped parts, the specified cutting conditions are not reached when the technological operation is set up for tools with a circular cutting edge. This is caused by the continuous change of contact point between the tool and the workpiece together with the fact that the cutting conditions are conventionally set to the tool reference point. Therefore, this paper contributes to the clarification of the feed rate control issue during point milling of complex–shaped parts and presents a feed rate optimization method to maintain a constant feed per tooth at the contact point along the entire toolpath. The proposed optimization method is based on the new derived relationship between the feed rate at the contact point and the feed rate at the tool reference point using the calculation of the actual pole of the movement of the tool reference point and actual pole of the movement of the contact point. This relationship is then used to recalculate the feed rate value at tool reference point to maintain the constant feed rate at contact point. The proposed method is then experimentally verified, and the advantages of applying this method are presented.

Keywords Feed rate · Feed per tooth · Contact point · Point milling · Complex shape

1 Introduction

Generally, in milling operations, the feed rate is specified at the tool reference point, i.e. the tool tip point (T_T). Figure 1 schematically shows climb milling of a contour where the tool performs a straight-line motion during 2D milling operation (the tool is shown in a section perpendicular to the tool axis). In this case, the prescribed feed rate to the tool centre is the same for each point on the tool, as indicated by differently coloured feed rate vectors. The red vector indicates the feed rate of the tool tip point (*vf*_TT) which is the same as the feed rate (*vf*) specified by technologist, while the black vectors indicate the identical feed rate of the remaining parts of the tool. The blue and purple vectors *vf*_OUT and *vf*_CP are identical in magnitude and direction to the other vectors, but are differentiated by colour and markings due to their importance in the subsequent clarification of consideration of the angular velocity's effect on the feed rate. The blue vector (*vf*_CP) represents the feed rate at the contact point of the tool with the workpiece (C_P). The purple vector (*vf*_OUT) represents the feed rate on the opposite side of the tool that is not in contact with the workpiece.

However, when machining circular segments or general curves, the situation is different. The feed rate is still programmed to the tool tip (that follows the circle of radius R_T), but due to the angular velocity, the tool tip moves at a different feed rate from the pole of movement compared to the "contact point" (that follows the circle of radius R_W) and "outside" of the tool (Fig. 2). At the contact point between the cutting tool and the contour of the workpiece, the feed rate prescribed by the programmer is not achieved. In other words, the feed rate per tooth, which is normally carefully selected to consider the tool's cutting edge life, is not observed, which can affect tool wear (especially when

✉ Petr Vavruska
p.vavruska@rcmt.cvut.cz

[1] Department of Production Machines and Equipment, Faculty of Mechanical Engineering, Czech Technical University in Prague, Technicka 4, 16607 Prague 6, Czech Republic

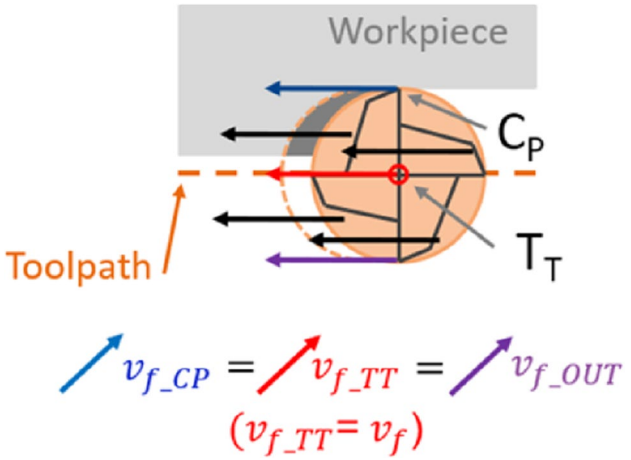

Fig. 1 Climb milling

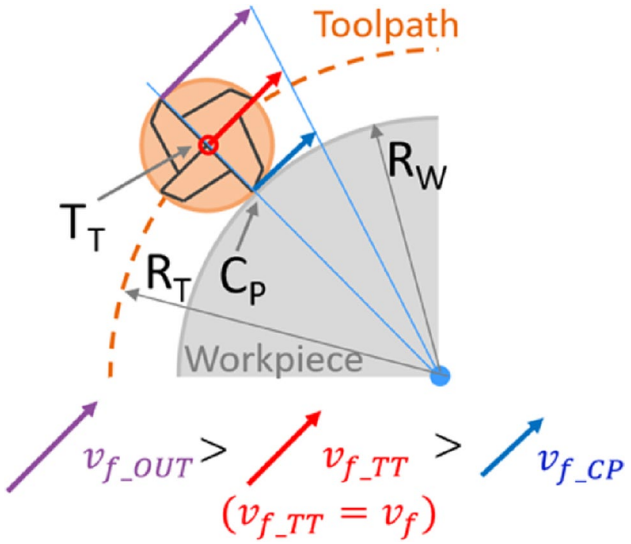

Fig. 2 Feed rate relationships when machining radii

machining difficult-to-machine materials), cutting stability and possibly deteriorate workpiece accuracy and surface quality.

In the context of the current state of the art of feed rate control, several areas related to feed rate control in milling were identified. The most comprehensive area is undoubtedly research into feed rate optimization aiming to achieve constant material removal or constant machining performance. Another area where feed rate control is applied is when a constant feed per tooth needs to be achieved due to the actual curvature of the toolpaths. A very extensive area is covered by papers focused on achieving smooth motion and therefore smooth feed rate changes by offline modification of toolpath points, i.e. modification that is performed before the NC program enters the control system. However, feed rate control must also be resolved at the level of NC program online processing directly in the control system, which is another extensive research area. Today, feed rate control is also applied at the level of digital twin machining. There are also applications using feed rate control to ensure a constant feed per tooth as a technological side effect when changing the spindle speed to achieve a constant cutting speed. The areas will now be analysed in more detail.

An analytical method of finding the characteristic of the actual engagement angle of 2.5D toolpaths was discussed by Gupta [1]. Using this method, the characteristic of the engagement angle was found to be of the same quality as using discrete simulation, which is used to verify toolpaths. Therefore, the determination of the engagement angle can be the basis for recalculating the feed rate. Uddin et al. [2] discuss an algorithm for modifying semi-finishing toolpaths to achieve constant performance during finishing machining. In their paper, they compare the benefits in accuracy achieved after machining and machining time. They compare the proposed method for 2D toolpaths with the conventional machining method, and in addition, they show a comparison with a method using feed rate control instead of toolpath modification. The authors also present the finding that during feed rate control, the desired feed rate is not achieved by the control system due to the setting of the machine axis drive parameters.

Ma et al. [3] indicate the importance of the shape of the workpiece surface on the appropriate toolpath geometry setting and achieving the resulting surface roughness. Therefore, they proposed a method to compute the toolpath geometry for a given workpiece surface shape which is based on the creation of tool feed vector maps. At each location on the workpiece surface, the height of the remaining material is determined both in the plane longitudinal to the tool motion and in the plane transverse to the tool motion direction. The optimum tool movement direction at the toolpath point is then selected based on achieving the minimum height of remaining material on the workpiece surface as determined by the tool feed vector maps. After a machining test, the achievement of a better surface roughness is evaluated using the proposed toolpath calculation method. However, the analysis of the characteristic of the actually achieved feed rates along the toolpath is not performed.

Bagri et al. [4] express in their work the importance of toolpath radius on tool life in micromachining. Therefore, they propose a method using neural networks to predict tool wear with consideration of tool runout. The input parameters include cutting forces, toolpath radius, depth of cut, feed, speed and also the actual tool wear condition as determined by measurement. The result is a prediction of the remaining tool life based on the input values. The outcome of the study is that the higher the toolpath radius, the lower the tool life. However, the causes are not discussed,

and the analysis of the feed rate characteristic is lacking. The method is suitable for planar machining.

Mali et al. [5] in their paper present a very extensive analysis of current approaches to the optimization of machining of complex-shaped parts. One of the important parameters for optimization is to maintain a constant material removal rate and maintain a constant tool load during machining, which has a positive effect on machining stability and the tool life. Modifying the toolpath to achieve a constant material removal rate has also been investigated for five-axis toolpaths, as shown, for example, by Liu et al. [6]. The scope of research in this case concerns toolpaths for machining inner corners by flank milling.

Ghorbani et al. [7] proposed a method to detect the intersection volume of tool and workpiece along the toolpath from CL data. The intersection is detected using nine toolpath points with one of these points being the current toolpath point, then one previous point, one next point, and then three points from the neighbouring toolpath on the right and three points from the neighbouring toolpath on the left. The cutting forces are then calculated based on the current material removal rate. The method is ready for machining with ball end mills. The advantage is the applicability of this method in CL data processing. The disadvantage of this method is very low accuracy for concave shapes which have high curvature.

An analytical method for calculating cutting forces suitable for curved toolpaths is presented by Zhang et al. [8]. Do et al. [9] demonstrated the importance of maintaining a specific feed rate value to obtain the desired roughness value Ra when machining a part made of hardened SKD 11 steel. Wu et al. [10] present two-step feed rate optimization. Firstly, based on the cutting force calculation model and the observed material allowance, a corrected feed rate characteristic is calculated to achieve constant cutting performance, and in the second stage, the feed rate characteristic is adjusted to produce smooth movements.

The neural network method was used by Xie et al. [11] to predict the spindle load characteristic in three-axis machining and then optimize the feed rate to achieve a smooth spindle load characteristic without abrupt changes. In their paper, Liu et al. [12] presented a position-oriented process monitoring method, which is based on calculating the actual material removal rate, predicting vibration and cutting power during machining, and then modifying the feed rate in an NC program. The advantages of this optimization are presented when the machining of two thin aerospace parts (one in aluminium alloy and the other in titanium). The method is unique in that it is based on the results obtained by synchronizing the sensed signals obtained directly from machining and the data regarding the tool position relative to the part from the NC program.

Park et al. [13] presented a feed rate control method based on achieving a constant cutting force, which they implemented directly into the specific control system of a newly developed machine tool. Offline feed rate recalculation based on the maximum allowable cutting force, which is calculated and modelled in dependence on the actual geometry of the toolpath and the material being removed, was presented by Hemmett et al. [14]. Ma et al. [15] presented another non-traditional approach to maintaining smooth cutting force changes where no feed rate control is used, but the design of toolpaths is such that changes in tool position relative to the part lead to smooth changes in the amount of material currently being removed. Qin et al. [16] proposed two feed rate control variants (continuous and discrete) to achieve better machining quality while reducing machining time. This method relies on the prediction of vibration during machining, but is limited to conical-shaped parts. The approach involves achieving the highest possible cutting force when the machining is stable.

A method for selecting the optimum spindle speed, cutting width and feed rate in three-axis machining was presented by Sun et al. [17]. This method is based on the principle of predicting the cutting forces and calculating the material removal rate per tooth and then predicting the machining errors, which must not exceed permitted values. Kiswanto et al. [18] present the effect of feed rate setting on burr formation during micromachining by performing machining tests. By adjusting the feed rate appropriately, burr formation can be prevented, and the quality of machining can be improved.

Erkorkmaz et al. [19] established algorithms for feed rate planning that also include the machine tool drive parameters. To achieve the smoothest feed rate changes, toolpath points are also replanned by approximating the points from CL data with spline curves. The result is a feed rate characteristic determined by the limits of the machine tool drives and the cutting forces.

García-Hernández et al. [20] deal with recalculation of feed rate when trochoidal toolpaths are realized. The feed rate value is then recalculated according to the angular movement of the tool along the toolpath. The equations used for feed rate control are prepared exactly for the 2D trochoidal toolpaths to respect the circular segments of movement. It is stated that the milling experiments performed on the CNC machine tool showed the slightly lower tool wear in the case when the feed rate is recalculated, but the measured values are not given. The method of achieving constant feed per tooth at contact point using feed rate control with respect to an angular velocity of the tool in 2D toolpaths in general is presented by Vavruska et al. [21]. They showed the positive effect of maintaining the constant feed per tooth by achieving of lower differences in the measured characteristic

of cutting forces than in the conventional case of milling. Krajnik et al. [22] presented feed rate optimization based on detection of the toolpath curvature radius combined with feed rate control capabilities in the control system. With this optimization, the desired feed rate is maintained.

In the work of Rahman et al. [23], iterative selection of feed per tooth, based on a cutting force constraint derived from a static tool deflection model and feed rate and tool length changes, is combined to calculate machining time. The results suggest potential machining time savings. The importance of achieving the necessary feed rate to maintain the required accuracy in micromachining was presented by Sodemann et al. [24]. They used a feed rate recalculation based on the actual toolpath radius in combination with an algorithm to appropriately segment the toolpath and approximate segments by a curve. Yau et al. [25] presented feed rate recalculation during interpolation using NURBS curves with consideration of the toolpath shape and machine dynamics settings.

Mayor et al. [26] presented two toolpath segmentation method solutions leading to increased machining efficiency. Both methods lead to an increase in feed rate and hence save machining time by adjusting the distribution of toolpath points to achieve smooth motion while controlling the machine tool drives. In order to eliminate sharp changes (discontinuities) in acceleration, an optimization method was developed by Zhang et al. [27] to generate a smooth toolpath based on the allowable tolerance. This method is based on the use of the third trajectory derivative, i.e. pseudo-jerk, as an optimization parameter to obtain a trajectory for smooth tool motion relative to the part. The method was designed and tested for two-axis control in the XY plane, where the jumps of abrupt change in acceleration were removed to achieve smooth motion. Chen et al. [28] presented the unit arc length increment scanning method (UALISM), which was developed to efficiently calculate and adjust the feed rate at the corners of complex toolpaths (defined by parametric curves). The calculation is based on an approximation that is dependent on the maximum allowable deviation and maximum defined velocity and acceleration of machine tool axes. Savings in machining time were achieved.

Research is also focused on interpolator solutions for control systems. Yeh et al. [29] proposed an interpolation method using adaptive feed rate control to reduce linear interpolation errors. The algorithm checks and ensures a specified error (deviation) limit on linear segments. Farouki et al. [30] proposed feed rate optimization (implemented in the control system) depending on the curvature of the machined surface. Pythagorean-hodograph (PH) curves were used for the solution. A reduction in cutting forces during machining was verified through experimental application of feed rate control.

Tikhon et al. [31] proposed a NURBS interpolator solution based on adaptive feed rate control to achieve a constant material removal rate. A reduction of cutting forces and increase in tool life using the proposed interpolator was experimentally demonstrated. An improved interpolator solution for controlling the feed rate along the toolpath was presented by Farouki et al. [32], where the coefficients of the third-degree Taylor polynomial were solved for refining. The authors mention that higher accuracy was achieved in reaching the toolpath, but they also state that interpolators using this calculation method will not achieve the same accuracy as interpolators using PH curves.

Tsai et al. [33] presented an algorithm that generates a time-dependent function to recalculate the feed rate (depending on the curvature of the paths) and uses the derivative of this function to control the magnitude of the feed rate change during machining. A feed rate control algorithm based on smoothing two consecutive curves to achieve smoothness of motion was presented by Zhang et al. in [34]. The proposed feed rate calculation is suitable for three-axis control and is capable of real-time operation, making it suitable for implementation in a control system. Sencer et al. [35] proposed a solution that is also based on achieving smooth tool motion; however, quintic Bézier blends with six control points are used to smoothly move between the linear toolpath movements. The authors mention the advantage of achieving G2 continuity compared to other solutions and thus achieving smooth feed rate control.

Ward et al. [36] proposed an advanced optimization loop using digital twin machining including real-time simulation. Both motion smoothness and vibration occurrence are predicted in this simulation, and spindle speed and feed rate control are optimized so that vibrations do not occur during machining. The use of this optimization method is demonstrated in the machining of a thin-walled part, where machining vibrations have been eliminated. Vavruska et al. [37] introduced a dynamic spindle speed control method together with feed rate control for milling with a circular cutting edge tool to achieve constant cutting speed. This paper outlines the benefits of the proposed method, such as achieving higher surface quality and reducing machine time. However, the feed rate control does not include the influence of the toolpath curvature. Käsemodel et al. [38] presented a surface speed optimization function for milling free-form shapes with a ball-end mill, which takes several parameters as inputs, such as normal vector, feed per tooth, programmed cutting speed, maximum spindle speed and the previously generated NC code. They developed stand-alone software to recalculate the surface speed for each machine tool position and when the RPM difference due to the effective tool diameter change was greater than 50 compared to the programmed value. Vavruska et al. [39] validated an extended

model for spindle speed control with respect to acceleration of the machine tool spindle. It was shown that the extension of the model by a specific value of spindle acceleration has a significant effect on the calculation of the feed rate in order to maintain a constant feed per tooth. It was also proven that spindle speed control has a significant effect on increasing tool life in milling operations.

Segonds et al. [40] proposed a new analytical model to predict the total scallop height taking into account the effect of the feed rate. The model is prepared for three-axis milling operations. It has been proven by the machining experiments that the prediction of scallop height does not deviate by more than 5% compared to the measured value. The model has been verified using the toolpaths used for milling the flat surface when the tool is tilted by specific angle. It has been stated that the feed rate has a significant effect on the scallop of machined surface. The proposed model has significant importance when preparing the setup of cutting conditions for point milling operations.

This overview shows that feed rate control is approached from many different perspectives. However, the effect of the toolpath shape itself on feed rate planning has thus far only been addressed in three papers, and only for 2D toolpaths. However, situations that are similar to the level of two-axis control and have been mentioned in [20] also occur in three-axis and multi-axis control. Thus, if the tool motion is not only linear, the angular velocity with respect to the current tool motion pole is also included in the resulting motion velocity at the contact point between the tool and the workpiece. To date, no literature has been found that deals with the calculation of the real feed rate at the contact point between the tool and the workpiece in three-axis and multi-axis control. No solution has been found so far that focuses on planning the feed along a three-axis or multi-axis toolpath to achieve a constant feed per tooth directly at the contact point. Therefore, this paper aims to present a method for calculating the real feed rate at the contact point between the tool and the workpiece and a method for correcting the feed rate to achieve a constant feed per tooth in milling operations. This means that the proposed method will consider the angular movement of the tool to recalculate the feed rate to achieve the constant feed per tooth directly in the contact point. The second objective pursued by this paper is to investigate the effects of this feed rate control during machining on the machine tool.

2 Calculation of the real feed rate at contact point

To calculate the actual feed rate at the contact point, it is necessary to proceed through the calculation of the ratio of actual radius of the pole of tool tip movement and actual radius to the contact point. If we focus on the movement between the toolpath points in three-axis control, this is linear movement (linear interpolation), but this would only really be true if the control was carried out in "exact stop" mode (control system mode), which would result in intermittent movement along the toolpath, which is undesirable when machining shaped surfaces because of the resulting surface smoothness and, of course, because of machining productivity. However, continuous three-axis control uses a mode in which many toolpath points are loaded forward (look-ahead mode), which allows the control system to calculate continuous feed rate changes along the toolpath, making the motion continuous rather than intermittent. However, the real tool motion is then distorted by the controller at partial toolpath points, i.e. the partial toolpath motions are no longer linear but form a continuous curve. This happens because of the continuous-toolpath mode (look-ahead mode) of the controller is used when point milling operations. Then, the same applies to the connection of the partial contact points between the tool and the workpiece at the partial toolpath points.

2.1 Pole of tool tip movement

When setting the finishing toolpath, the technologist defines the feed rate, which is realized on the toolpath, i.e. at the tool reference point. However, the tool is not in contact with the workpiece at the tool reference point, but at a contact point that is constantly moving on the tool ball end profile. The contact point therefore also creates a path in the form of a curve during tool movement according to the workpiece surface shape. Figure 3 shows two positions of the tool relative to the workpiece when point milling of the complex shape. In fact, it is not needed to maintain the feed rate at the tool tip point (point T_T in Fig. 3), which is specified by the technologist, but it is needed to maintain the feed rate at the actual contact point between the tool and the workpiece (i.e. C_P in Fig. 3). This is the only way to maintain the feed per tooth, which needs to be kept at a constant value in terms of cutting conditions. If the radius of curvature of the contact point path and the radius of curvature of the tool tip movement (pole of motion) are known, the ratio of these dimensions can be used to recalculate the feed rate from the tool tip point to the contact point between the tool and the workpiece. This issue arises in all cases of point milling using cutting tools with a circular cutting edge (ball-end mills, toroidal mills, tapered mills with a ball end, etc.). Therefore, the equations mentioned below, which will be used for further calculations, will be applicable for the use with tools with a circular cutting edge in general. The issues are similar for multi-axis machining cases. By the fact that in such cases the orientation of the tool relative to the part changes, it

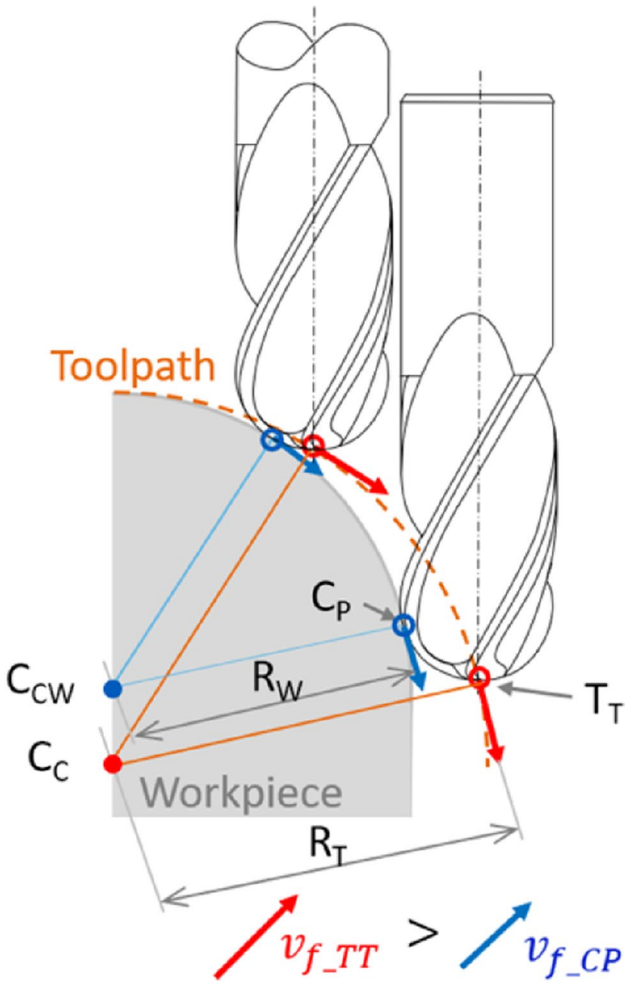

Fig. 3 Tool movement relative to the workpiece when radius surface machining

is necessary to take into account the unit vector (which determines the orientation of the tool axis in space) in some of the calculations. According to the fact mentioned in the first paragraph of this chapter, the actual radius of the movement (pole of motion) at a given toolpath point can be calculated from the toolpath points.

One possible solution for determining the radius of movement would be to use the standard calculation of a circle from three consecutive points in the toolpath. However, there is a difficulty here which lies in the way each CAM system calculates toolpath points, i.e. it calculates linear interpolations within a certain envelope (defined by the tolerance value) around the ideal toolpath curve to achieve a certain minimum required number of toolpath points. The result may be, for example, that shown in Fig. 4, which also has implications for the toolpath points, e.g. this has the effect that if we determine a circle at a certain toolpath point (T_{Tn}) from the current three consecutive points (T_{Tn-1}, T_{Tn}, T_{Tn+1}), its radius is different than that of a circle that

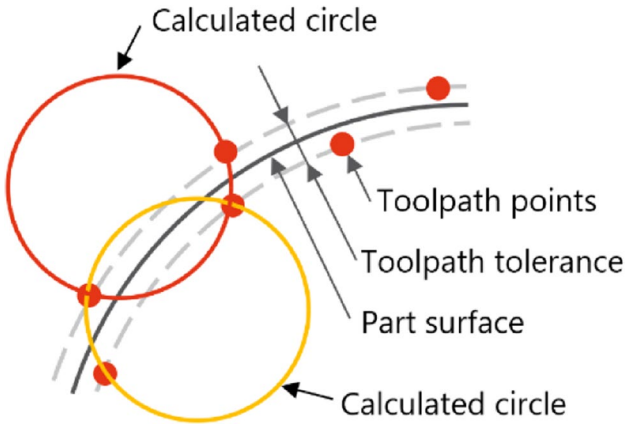

Fig. 4 Computational error in three-point circle calculation

we construct immediately at the next point of the toolpath (T_{Tn+1}) from the next three points (e.g. T_{Tn}, T_{Tn+1}, T_{Tn+2}). The radius should be the same. Through linear interpolation of the curve, the radii of successive circles are slightly varied, and thus the result is not a smooth change.

Therefore, the proposed solution would reduce the influence of the positional error of the generated points from CAM by adding more points to the circle calculation algorithm, and thus the resulting circle would be a best fit approximate to the provided set of points. Six toolpath

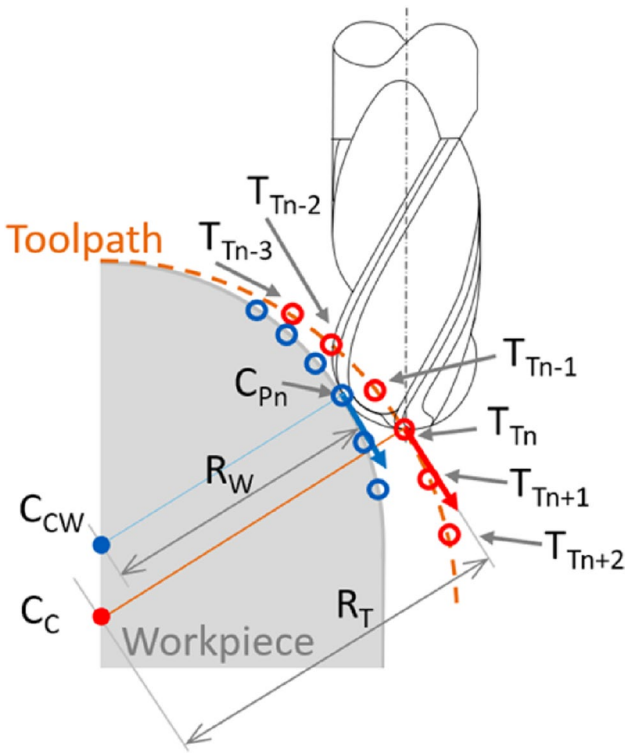

Fig. 5 Points used for the calculation

points T_{Tn-3}, T_{Tn-2}, T_{Tn-1}, T_{Tn}, T_{Tn+1} and T_{Tn+2} (Fig. 5) have been selected as surely sufficient number of points. The toolpath tolerance is used to be very narrow (e.g. 1–6 µm) when finish milling of complex-shaped surfaces to achieve enough points to make the toolpath as smooth as possible; therefore, the six points are very close together, and the radius can be reliably calculated also on curvature transitions. The best fit would be calculated using the least squares, which gives a good compromise between computational efficiency and accuracy. The needed output would once again be the circle centre coordinates and its radius.

To be able to find the best fit circle, all the input points must lie on the same plane since a circle is a 2D shape. However, the outputted points from the CAM software may not always lie on the same plane, either because of the positional error caused by the toolpath tolerance or simply because of the shape of the toolpath/workpiece curvature. This needs to be resolved first before computing the best fit circle using the best fit plane as a numerical approximation from the provided set of tool tip points. Once the best fit plane equation has been found, the input set of tool tip points is projected into the best fit plane, and the best fit circle can be calculated using these points. The best fit circle algorithm is used to compute the circle centre and its radius R_T. The next step is to compute the radius R_W the same way as well. The ratio of radius R_W and radius R_T will be the compensation coefficient for the optimized feed rate.

2.2 Best fit plane calculation

The goal is to find a plane that will lie as close as possible to a set of k 3D points (P_1, …, P_k) which are in fact the points (T_{Tn-3}, T_{Tn-2}, T_{Tn-1}, T_{Tn}, T_{Tn+1}, T_{Tn+2}) when calculating R_T, respectively (C_{Pn-3}, C_{Pn-2}, C_{Pn-1}, C_{Pn}, C_{Pn+1}, C_{Pn+2}) when calculating R_W. The best fit plane can be found using least square method. At first it is evaluated based on the sum of the squared orthogonal distances between the plane and the points. Let the plane be described by a point C belonging to the best fit plane and a unit vector $\vec{n}$, which is the normal to the plane. The orthogonal distance between a point P_i and the plane is then $\left(P_i - C\right) \cdot \vec{n}$. The plane can then be found by solving (1), (2) and (3). To find a best fit plane, a criterion (1) must be adhered to. Point C is defined by (2). A matrix (3 x k) marked by A is defined as (3). The plane unit normal vector $\vec{n}$ and plane base vectors $\vec{v}_{base1,2}$ are given by solving the singular decomposition $A = USV^T$, where U is a unitary matrix, S is rectangular diagonal matrix and V is complex unitary matrix. The outputs $\vec{v}_{base1} = U(:,1), \vec{v}_{base2} = U(:,2)$ and $\vec{n} = U(:,3)$ are needed to define the best fit plane.

$$\min_{C,||n||=1} \sum_{i=1}^{k} \left(\left(P_i - C\right) \cdot \vec{n}\right)^2 \tag{1}$$

$$C = \frac{1}{k} \sum_{i=1}^{k} P_i \tag{2}$$

$$A = \begin{bmatrix} P_{1(x)} - C_{(x)} & P_{2(x)} - C_{(x)} & \dots & P_{k(x)} - C_{(x)} \\ P_{1(y)} - C_{(y)} & P_{2(y)} - C_{(y)} & \dots & P_{k(y)} - C_{(y)} \\ P_{1(z)} - C_{(z)} & P_{2(z)} - C_{(z)} & \dots & P_{k(z)} - C_{(z)} \end{bmatrix} \tag{3}$$

2.3 Best fit circle calculation

Once the best fit plane is known, the input set of k 3-D points (P_1, …, P_k) must be projected into this plane. A directional vector $\vec{v}$ for each point P is calculated as $\vec{v}_i = P_i - C$.

The directional vector $\vec{v}$ is then transformed from 3D into 2D coordinates using a 2 × 3 transformation matrix T as $\vec{v}_{2D_i} = T\vec{v}_i$. The transformation matrix is defined as $T = \left[\vec{v}_{base1}, \vec{v}_{base2}\right]^T$.

The transformed directional vector $\vec{v}_{2D}$ elements also represent the 2D coordinates of the 3D point in the best fit plane.

Given a finite set of points in $\mathbb{R}^2$, the next step is to find a circle that best fits the points. The general circle equation in $\mathbb{R}^2$ formed as (4), where x_0 and y_0 are the coordinates of circle centre, can be also simplified using (5) and (6). The equation for multiple input points can be written in the matrix form as (7).

$$\left(\vec{v}_{2Di(x)} - x_0\right)^2 + \left(\vec{v}_{2Di(y)} - y_0\right)^2 = R_T^2 \tag{4}$$

$$2 \cdot \vec{v}_{2Di(x)} \cdot x_0 + 2 \cdot \vec{v}_{2Di(y)} \cdot y_0 + r = \vec{v}_{2Di(x)}^2 + \vec{v}_{2Di(y)}^2 \tag{5}$$

$$r = R_T^2 - x_0^2 - y_0^2 \tag{6}$$

$$\begin{bmatrix} 2 \cdot \vec{v}_{2D1(x)} & 2 \cdot \vec{v}_{2Di(y)} & 1 \\ \vdots & \vdots & \vdots \\ 2 \cdot \vec{v}_{2Dk(x)} & 2 \cdot \vec{v}_{2Dk(y)} & 1 \end{bmatrix} \begin{bmatrix} x_0 \\ y_0 \\ r \end{bmatrix} = \begin{bmatrix} \vec{v}_{2D1(x)}^2 + \vec{v}_{2D1(y)}^2 \\ \vdots \\ \vec{v}_{2Dk(x)}^2 + \vec{v}_{2Dk(y)}^2 \end{bmatrix} \tag{7}$$

$$\begin{bmatrix} 2 \cdot \vec{v}_{2D1(x)} & 2 \cdot \vec{v}_{2Di(y)} & 1 \\ \vdots & \vdots & \vdots \\ 2 \cdot \vec{v}_{2Dk(x)} & 2 \cdot \vec{v}_{2Dk(y)} & 1 \end{bmatrix} = B \qquad \begin{bmatrix} x_0 \\ y_0 \\ r \end{bmatrix} = \vec{d} \begin{bmatrix} \vec{v}_{2D1(x)}^2 + \vec{v}_{2D1(y)}^2 \\ \vdots \\ \vec{v}_{2Dk(x)}^2 + \vec{v}_{2Dk(y)}^2 \end{bmatrix} = \vec{b} \tag{8}$$

To simplify the notation, the matrix and vectors from the system of Eq. (7) can be labelled as (8). The system of linear equations $B\vec{d} = \vec{b}$ does not have an exact solution unless it is calculated with exactly three points ($k = 3$). To find the approximate solution, it means to find $\vec{d}^*$ (complex conjugate of $\vec{d}$) using (9) and (10). The equation can be solved by matrix inversion using (11).

$$\min \left\| \vec{b} - B\vec{d}^{*} \right\| \tag{9}$$

$$\mathrm{B}^{\mathrm{T}} B\vec{d}^{*} - B^{T}\vec{b} = 0 \tag{10}$$

$$\vec{d}^{*} = \left(B^{T}B\right)^{-1}\left(B^{T}\vec{b}\right) \tag{11}$$

The results are the circle centre coordinates x_0, y_0 and the value r, from which is the circle radius R_T calculated using (6).

The radius R_W is then calculated exactly the same way as the radius R_T; however the points (C_{Pn-3}, C_{Pn-2}, C_{Pn-1}, C_{Pn}, C_{Pn+1}, C_{Pn+2}) instead of (T_{Tn-3}, T_{Tn-2}, T_{Tn-1}, T_{Tn}, T_{Tn+1}, T_{Tn+2}) are used now for calculation, so R_W replaces now the R_T in (4), (5) and (6).

3 Algorithm and feed rate optimization

The optimization is based on calculating the circle radius from six consecutive tool tip points, which are defined by the toolpath and circle radius (respectively contact points). The computed circle radius R_T can be compared to the radius R_W, and the radius ratio of these two values is calculated. The radius ratio tells whether the part surface is convex or concave (Fig. 6).

The recalculation of feed rate to get the optimized value is based on considering the angular speed of the tool movement. The calculation of the feed rate at the contact point is simply derived from the fact that the tool tip point and the contact point have to change their´s positions when the tool is moving between the toolpath points in the same time period (t_{blk}). The angular velocities of movement of the contact point and tool tip are different. Since we know the centre of the circle that defines the motion of the contact point and the two consequent contact points (C_{Pn-1}, C_P), then we also know the angle that defines the change in position of the contact point (δ_{CP}). Since we know the centre of the circle that defines the motion of the tool tip and the two consequent tool tip points (C_{Pn-1}, C_P), then we also know the angle that defines the change in position of the tool tip (δ_{TT}). These parameters are seen in the Fig. 7. The time period t_{blk} is then defined by Eq. (12):

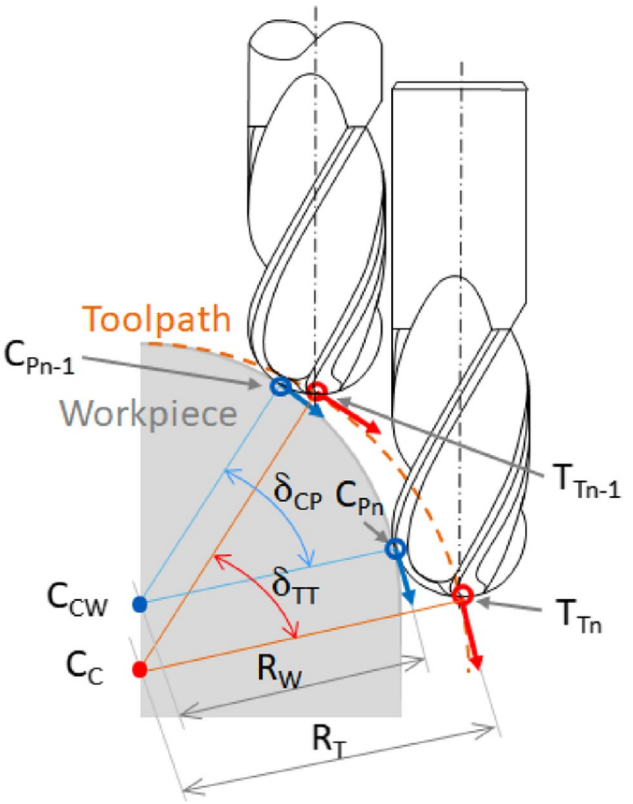

Fig. 7 Parameters needed for recalculation of feed rate

$$t_{blk} = \delta_{CP}/\varpi_{CP} = \delta_{TT}/\varpi_{TT} \tag{12}$$

The angular velocity of the contact point (ϖ_{CP}) and angular velocity of the tool tip point (ϖ_{TT}) are defined by (13) and (14):

$$\varpi_{CP} = v_{f_{CP}}/R_W \tag{13}$$

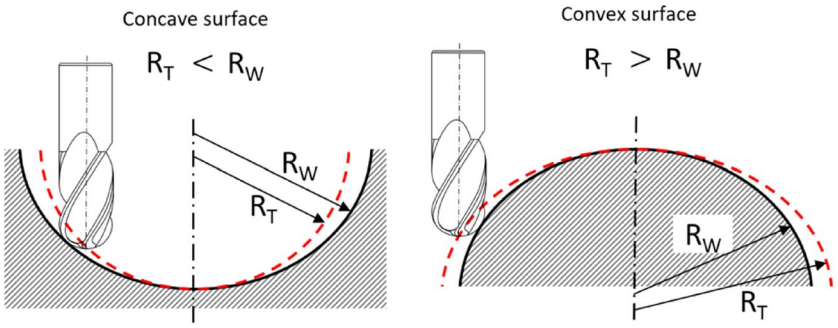

Fig. 6 Convex and concave milling difference

$$\varpi_{TT} = v_{f_{TT}}/R_T \tag{14}$$

The exact value of feed rate specified by the technologist is needed to be achieved directly in the contact point. This means that the v_{f_CP} has to be considered as this is the value of v_f, which is the specified value of feed rate and the v_{f_TT} is the value that is needed to be recalculated because this is the value generated to the NC program.

The optimization function then calculates the new programmed (optimized) feed rate, which is obtained using a radius ratio, the angles ratio and the programmed feed rate v_f (15). This equation is obtained by substituting Eqs. (13) and (14) into Eq. (12).

$$v_{f\_opt} = v_{f\_TT} = \left(R_T/R_W\right) \cdot \left(\delta_{TT}/\delta_{CP}\right) \cdot vf \tag{15}$$

However, by recalculation of the feed rate to maintain a constant feed per tooth in the contact point, not all the necessary cutting conditions, which affect the resulting qualitative and performance parameters achieved during machining, are maintained. The value of the cutting speed has a very significant influence. As mentioned in the introduction, when machining shaped parts by tools with circular cutting edge, the cutting speed at the contact point is not maintained as well [35]. Therefore, the optimization algorithm was extended by first calculating the real cutting diameter of the tool based on the contact point and also the required spindle speed to maintain a constant cutting speed.

Real cutting radius of the tool is calculated using (16), where C is the contact point, S_C is the centre of ball end mill and $\vec{e}$ is the unit vector of tool axis. The optimized spindle speed is then calculated as (17), where v_c is the desired cutting speed. Feed rate is then calculated by (18) where f_z is feed per tooth and z is the number of teeth.

$$R_R = \left|\left[S_C + \left|\left(C_P - S_C\right) \cdot \vec{e}\right| \cdot \left(-\vec{e}\right)\right] - C_P\right| \tag{16}$$

$$S_{opt} = \left(1000 \cdot v_c\right)/\left(2 \cdot \pi \cdot R_R\right), where: v_c \; is \; in \; \left[m/\min\right] \; and \; R_R \; is \; in \; [mm] \tag{17}$$

$$v_f = f_z \cdot z \cdot S_{opt} \tag{18}$$

3.1 Optimization algorithm

The algorithm of the new proposed feed rate optimization function based on the calculations mentioned above can be seen in Fig. 8. It can be seen that the algorithm checks if the three consequent toolpath points (T_{Tn-1}, T_{Tn}, T_{Tn+1}) form a line (if the two consequent toolpath movements form a line), where the optimization is not applied.

The proposed optimization function can be used in three options. The first option is used to optimize only the feed rate to keep the feed per tooth constant, the second option is used to optimize the spindle speed, and also the third option is used when combining the feed rate optimization with spindle speed optimization is needed to keep the feed per tooth constant as well as the cutting speed constant (Fig. 9).

3.2 Effect of optimization on feed rate

The algorithm mentioned above is programmed and directly implemented into the postprocessor as depicted in Fig. 10 for simply usage after creating the toolpath in the CAM system. In order to be able to observe how feed rate changes are distributed along the toolpath prepared in the CAM system, an algorithm was adopted so that the postprocessor generates not only the NC program, but also an optimized CL data file that can colour the toolpath in CAM system to display the feed rate values. This makes it possible to see the feed rate changes that occur along the toolpath so that a constant feed per tooth is maintained at the point of contact between the tool and the workpiece. This is a benefit for the technologist, who can verify and possibly rearrange the toolpath in regard to specific needs. This is only a secondary functionality; the main functionality is the generation of optimized NC program, where the cutting conditions are automatically optimized without requiring any additional action from the technologist. This means that no toolpath modifications are needed.

As previously mentioned, the weakness of the first simple circle calculation method relates to computational accuracy because of the three input points as shown in Fig. 4. A demonstrative geometry has been selected and is shown in Fig. 11 along with the feed rate values for the generated toolpath (cyan curve). The first way based on computing the circle using three points gives the feed rate characteristic represented by the blue curve. This characteristic tends to oscillate around the correct values. The feed rate values obtained from the proposed algorithm based on the best fit circle gives a smooth characteristic, which is represented by the orange curve. The characteristics are obtained for the required feed rate set on the value of 300 mm/min, which is the conventional feed rate value (represented by grey line). In general, there are three sections on the sample toolpath where the optimization of feed rate is needed. The sections are marked by the Roman numerals (I, II, III). Two sections marked by I and III are the sections where the reduction of feed rate is needed, because of the concave surface. However, the section marked by II needs primarily the

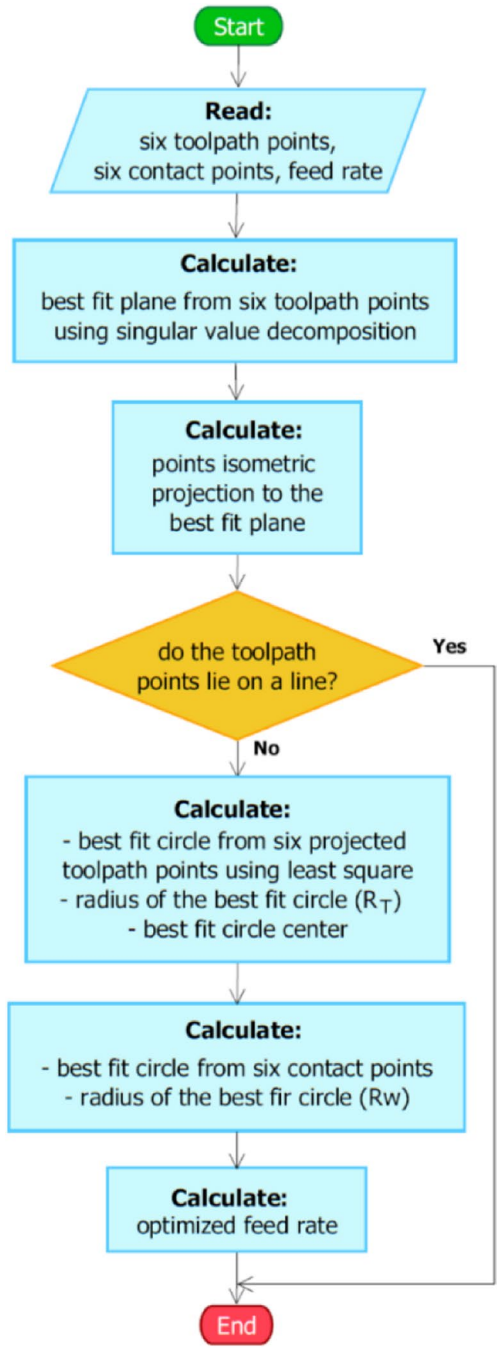

Fig. 8 Feed rate optimization algorithm flowchart

increase of feed rate because it is the convex surface, but the decrease of feed rate is needed as well, because of the influence of the actual angles ratio (according to the Eq. (15)).

This simply shows the possibility of using the proposed feed rate calculation method in practice. Only the method based on computing the best fit circle will be used from this point onwards.

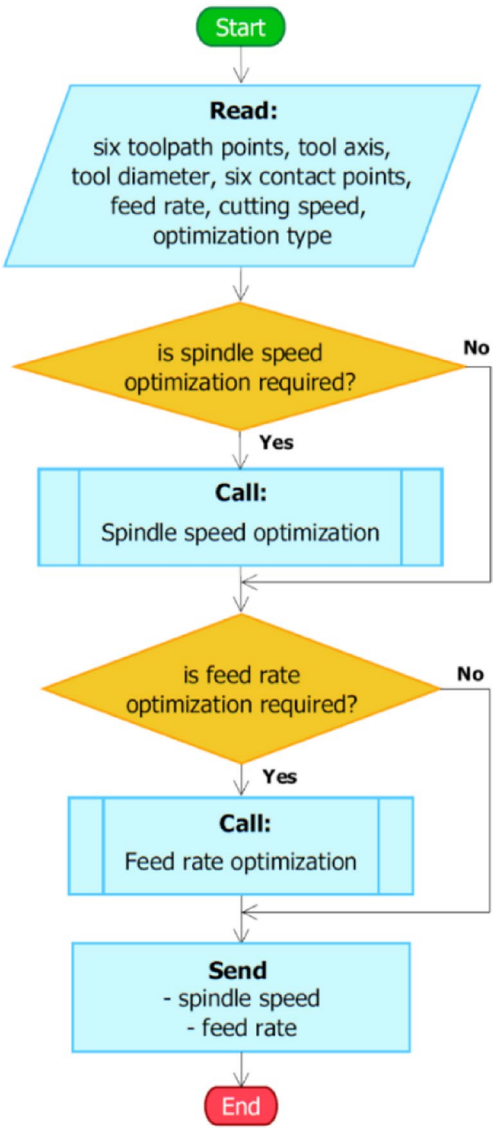

Fig. 9 Combined optimization function

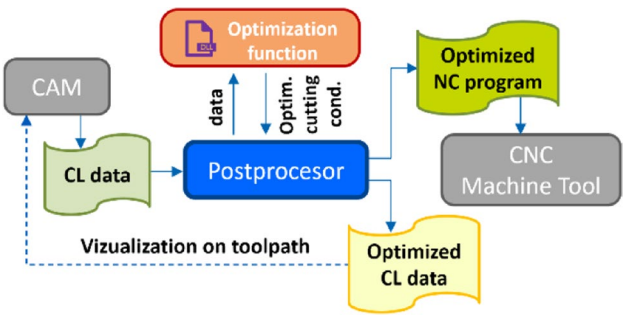

Fig. 10 Postprocessing workflow with implemented feed rate optimization function

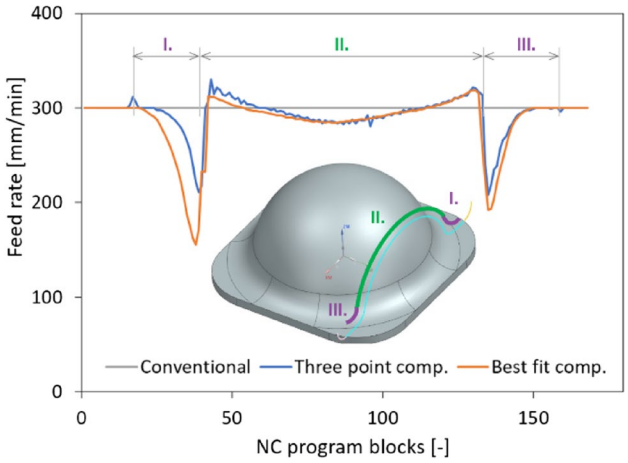

Fig. 11 Comparison of the two methods of computing the feed rate characteristics

4 Experimental verification

The intention is to analyse the benefits of the proposed optimization method on the real effects of the new optimization function on the real feed rate characteristic on the machine tool, tool life, energy consumption and roughness.

Therefore, two parts were chosen for testing purposes. In principle, they consist of one and the same surface (Fig. 12), but in the first case, the surface will be machined from the concave side and in the second case from the convex side. Given the shape and the toolpath, it is convenient to demonstrate the advantages, differences and potential of the optimization method.

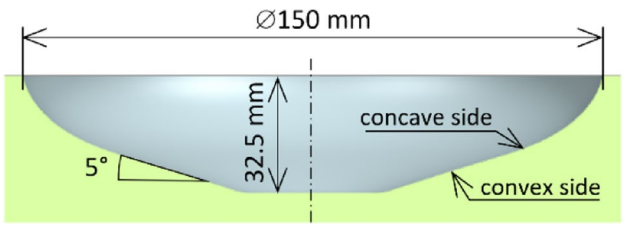

Fig. 12 Selected profile of surface for testing

The tool used for the finishing operation was a 16-mm 2 teeth ball end mill, the cutting speed set in CAM was 70 m/min, and the feed per tooth was 0.1 mm. These cutting condition settings lead to a conventional feed rate value of 278.6 mm/min. These cutting condition settings were selected because of the subsequent test performed on the machine tool, which entailed milling a bowl-shaped mould (Fig. 17) made of difficult-to-cut stainless steel 1.4462 as the testing part.

4.1 Analysis of the effect of optimization on feed rate control

First, the influence of the part shape or the toolpath on the feed rate control is analysed, taking into account the angular velocity. First, only the calculated feed rate is investigated, and then the real feed rate achieved by the control system on a real machine tool is examined.

The application of this feed rate control is demonstrated on machining operations for finish milling. The finishing operations are set up so that the toolpath points are interpolated only in the X-Z plane in each pass, and the Y-axis is applied only to the transition sections between the subpasses. The coloured toolpaths according to the calculated feed rates used for the NC programs for finishing machining of the selected surfaces for testing are shown in Fig. 13 (left for concave surface, right for convex surface). According to the displayed feed rate profiles, the differing influence of the shape of the machined surface or toolpath on the resulting feed rate can be seen. As the figure shows, in curved sections of the toolpath, the feed rate is modified and depends on where the contact point between the tool and the workpiece is located in relation to the toolpath. The green colour indicates where the newly calculated feed rate is practically the same as the conventional feed rate value. Locations where the tool must achieve a higher feed rate than the conventional value rate are marked in graduated shades of yellow to deep red. Locations where the tool must achieve a lower feed rate than the conventional rate value are indicated by shades of blue to black. It is evident that these areas are reciprocal for the convex and concave surfaces.

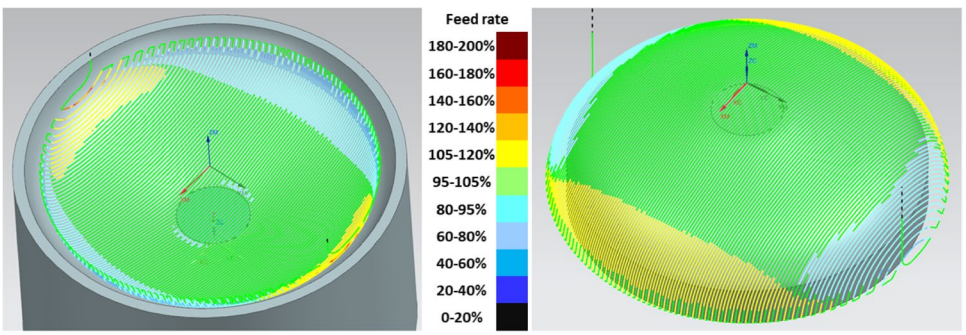

Fig. 13 Coloured toolpaths to vizualise percentual optimized feed rate changes

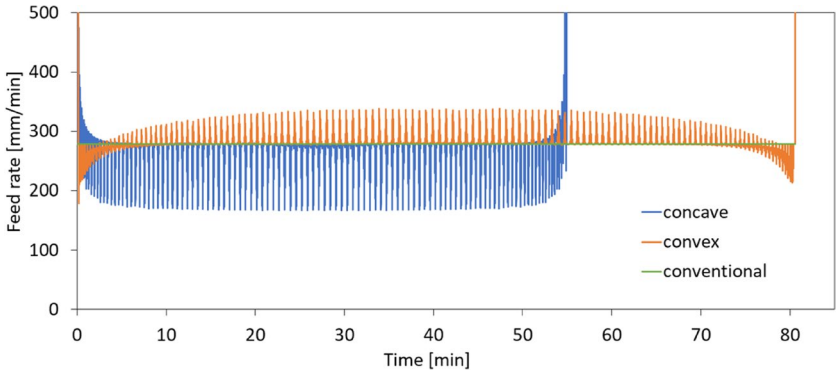

Fig. 14 Comparison between feed rate characteristics

Figure 14 shows a graph depicting the feed rate profiles for the entire toolpath for both the convex and the concave surfaces, but also shows the conventional feed rate value. As can be seen, for most of the toolpath in the convex surface case, the tool is forced to accelerate to achieve a constant feed per tooth, while in the concave surface case, the tool is forced to decelerate. The graph shows the individual passes within the total toolpath by the partial feed rate peaks. The conventional feed rate value is achieved at the areas of the passes between the partial cutting motions of the tool which are the areas where the path curvature approaches a flat section. While it may appear from this graph that there are sharp increases in feed rate, in fact there are not. As can be seen from the whole characteristic, about 15 peaks per 10 min are achieved, which means a time of about 40 s per period between two peaks. This is not a challenging task for the control system and the machine tool. However, the achievement of realistic feed rates for toolpath subsections will be further analysed.

4.2 Measurement of feed rates directly in the machine tool control system

A Tajmac ZPS MCFV 5050 LN 3-axis milling machine tool with a Sinumerik 840D control system was chosen for testing purposes. This machine tool is equipped with a spindle with a maximum spindle speed of 15000 RPM and ISO 40 tool interface.

It was necessary to verify whether the machine and the control system will actually be able to achieve the desired feed rate changes when executing the NC program. Therefore, one toolpath subsection was prepared on both types of surfaces, and for this toolpath, an NC program was generated with an optimized feed rate, i.e. feed rate changes on each block of the NC program. Four values of the basic (conventional) feed rate were chosen: 278.6, 500, 1500 and 3000 mm/min, i.e. commonly used feed rate values.

The toolpath for machining the concave surface is shown in Fig. 15a. The measured and programmed feed rate characteristics are then shown in Fig. 15b–e. The measured feed rate values show that the control system is able to maintain the change in programmed feed rate as required for optimization during actual machining. Machining times for conventional control of feed rate and also for optimized feed rate control were obtained from controller as well. The comparison of machining times is shown in Table 1, and it is clearly seen that the machining times are higher in the case of optimized control of feed rate because of the concave surface, where the maintaining of constant feed per tooth needs to reduce feed rate at certain sections of toolpath.

The toolpath for machining a convex surface is shown in Fig. 16a. The measured and programmed feed rate profiles are then shown again in Fig. 16b–e. From the measured feed rate values, it is again evident that the control system can maintain the change in programmed feed rate as required for optimization during actual machining. The actual measured feed rate characteristic in Fig. 16e shows that the control system at 3000 mm/min has some difficulty in maintaining the feed rate at the required value at the very beginning and at the end of the path. This is due to the path geometry itself, i.e. the distribution of toolpath points and machining at such a high feed rate. These changes are not affected by feed rate optimization, as it is clear that this occurs in sections where no change in feed rate is required. Machining times for conventional control of feed rate and also for optimized feed rate control were obtained from controller as well. The comparison of machining times is shown in Table 2, and it is clearly seen that the machining times are lower in the case of optimized control of feed rate because of the convex surface, where the maintaining of constant feed per tooth needs to increase feed rate at certain sections of toolpath.

Therefore, these tests show that machining optimization can be applied in real machining and the feed rate changes will be implemented by the control system as required.

4.3 Tool life test

Tool life test was performed on the bowl-shaped mould (made of difficult-to-cut stainless steel 1.4462), which consists of the concave surface (Fig. 12) mentioned above. All

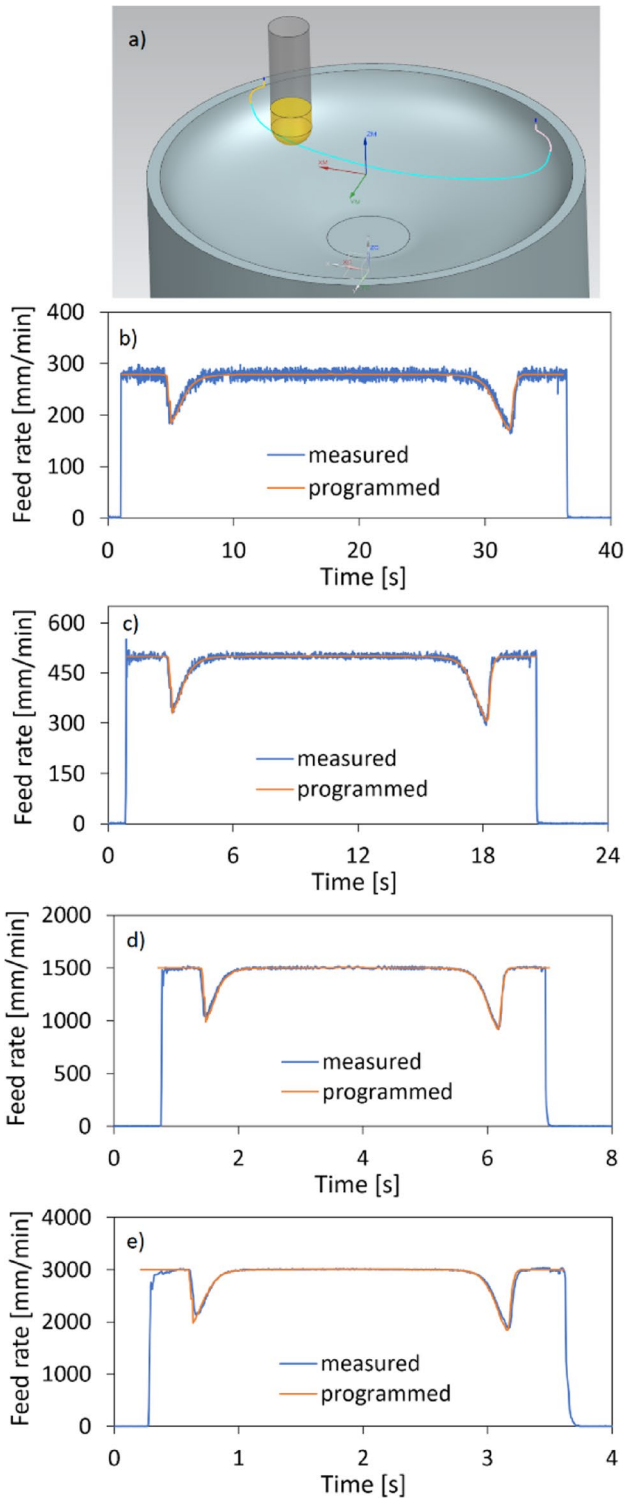

Fig. 15 Comparison of measured and programmed feed rates when milling concave shape

the milling cases were performed (conventional, feed rate optimization, spindle speed optimization, spindle and feed rate optimization).

Table 1 Machining time of one concave shape toolpath

	Machining time		
Feed rate [mm/min]	Conventional [s]	Optimized [s]	Difference [%]
279	34.28	35.36	+ 3.16
500	19.13	19.71	+ 3.03
1500	6.08	6.16	+ 1.28
3000	3.29	3.35	+ 1.57

A Rotana R-14154 solid carbide ball end mill with two teeth, 16 mm diameter, helix angle of 40° and RotalH coating was used for the finishing operation. The workpiece was clamped in a three-jaw-chuck as seen in Fig. 17.

The selection of initial cutting conditions was primarily driven by the tool producer based on the machineability of the material. The cutting speed was set at 70 m/min and feed per tooth was set at 0.1 mm. Flood cooling was used for this experiment.

First, the workpiece was roughened so that finishing operations could be performed. The finishing operations were repetitions created by shifting the *Z*-axis by the height of the remaining material (0.2 mm). After each shape was milled (as a layer) on the workpiece, the tool was removed from the spindle and inserted with the tool holder into the fixture on the Keyence VHX-7000 microscope, where the wear on both cutting edges was measured. The maximum cutting edge wear on the flank, noted as VB_{max}, was evaluated. The machining was repeated until the wear value VBmax reached 200 µm on one of the tool blades.

Figure 18 shows an example of a tool cutting edge wear comparison after milling the same area, specifically after machining of eight layers, i.e. 18.72 dm^2, each by one specific tool. The wear comparison shows that the tool that had been milling using the conventional NC program is at the end of its life as so in the case of feed rate optimization, while the tool that had been milling using NC programs based on the spindle speed optimization shows wear (VB_{max}) of the cutting edge on the value of 157 µm. The tool that had been milling using NC programs based on combined optimization of feed rate and spindle speed shows the lowest value of cutting edge wear (VB_{max} = 120 µm).

By observing the wear in more detail, a difference between the conventional case and the feed rate optimization can be found too. In the case of feed rate optimization, the chipping near the cutting edge is less noticeable and more uniform.

The cutting edge wear is most noticeable at the diameter that corresponds to the largest area of the toolpath, which is located on a section of the machined surface with an inclination of approximately 5°. The machining test results are shown in Table 3. Based on the feed

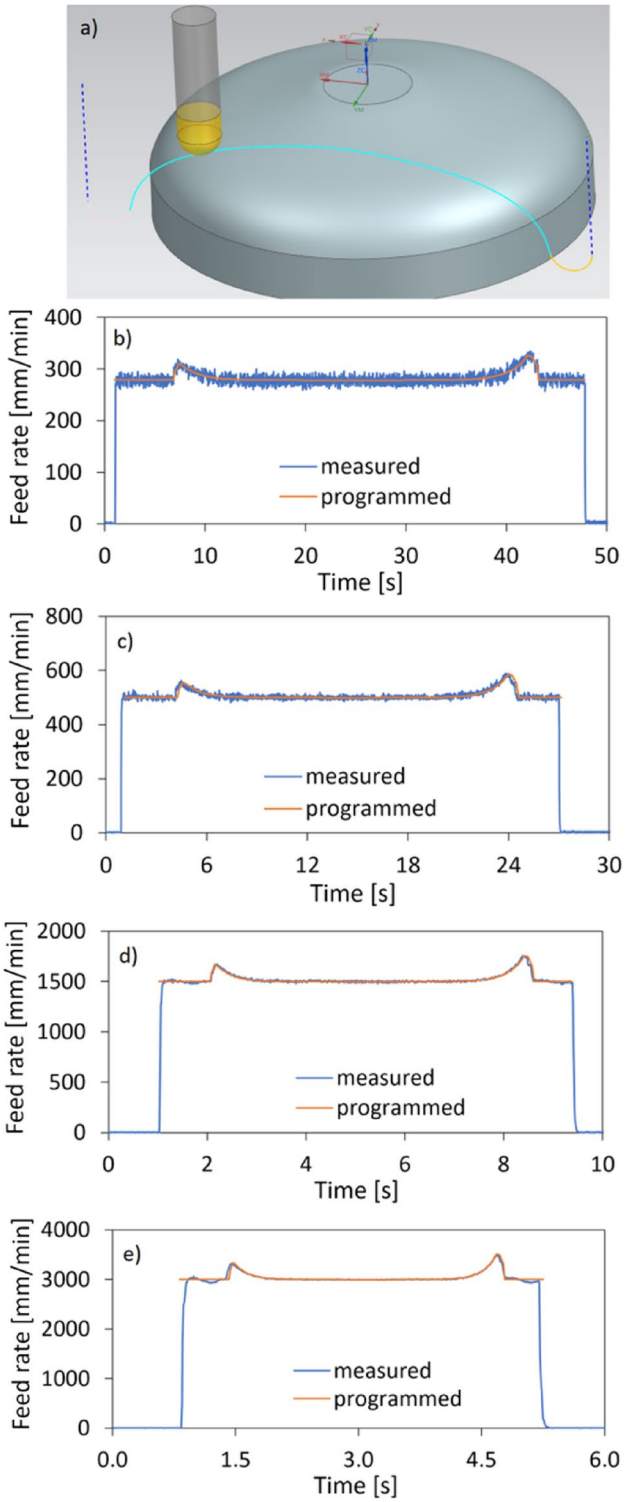

Fig. 16 Comparison of measured and programmed feed rates when milling convex shape

rate optimization principle of keeping the feed per tooth constant, the machining time with feed rate optimization is longer (55 min) than the conventional (53 min). The

Table 2 Machining time of one convex shape toolpath

	Machining time		
Feed rate [mm/min]	Conventional [s]	Optimized [s]	Difference [%]
279	48	46.81	− 2.47
500	26.81	26.15	− 2.47
1500	9.39	8.43	− 10.15
3000	4.97	4.46	− 10.31

Fig. 17 Machining setup

machining time using the spindle speed optimization is the lowest (26 min), because the spindle speed optimization increases the spindle speed to keep the cutting speed constant and the feed rate is recalculated too according to actual spindle speed value. The machining time using the combination of both optimizations (spindle speed and feed rate) is little higher (27.5 min) compared to the spindle speed optimization, because of the achieving the constant feed per tooth on concave surface. However, the benefit of combined optimization is prolonged tool life because the tool has milled 25 surfaces per tool life, which is more than four times higher tool life compared to the first two cases (conventional and feed rate optimization), and compared to the spindle speed optimization case, it prolonged the tool life by two more surfaces machined.

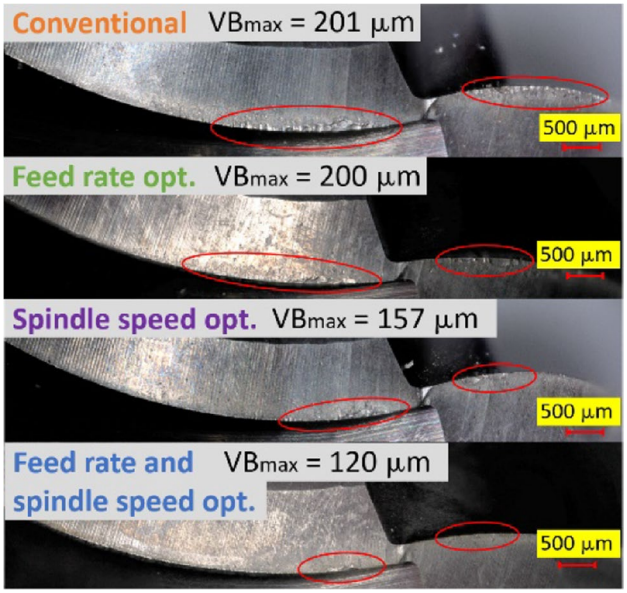

Fig. 18 Comparison of cutting edges of three machining options (after 8 machined layers)

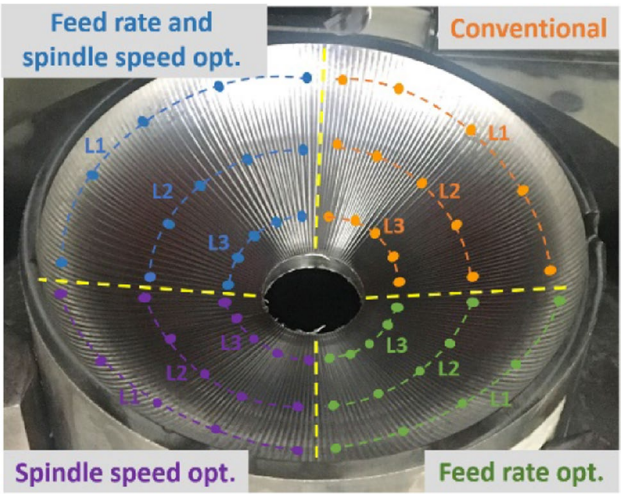

Fig. 19 Setup for roughness measurement

4.4 Surface roughness measurement

In order to compare machined surface roughness under different cutting conditions, the milling was carried out so that the toolpaths were adjusted to face the centre of the part. This made it possible to mill one layer of the part divided into four segments so that roughness could be measured on one machined layer. The division of one machined layer into four segments is shown in Fig. 19.

Surface roughness measurements were carried out in the direction of tool movement (along the toolpath–longitudinal roughness) at three different levels (marked L1, L2 and L3 in Fig. 17) on the machined surface for each of the four surface sections of the surface machined under different cutting conditions' control options. Five measurements were made at each level, which means 15 measurements per surface (the points are visible in Fig. 19). The roughness measurements were carried out using a Mahr LD130. The averaged measured values for each surface are shown in Table 4.

Ra values are surely the most frequently used parameter for evaluation of whether a machined surface achieves the required roughness. It is evident that the Ra values are nearly the same for the conventional and feed rate optimization variants, but the Ra value is lower for spindle speed optimization, and lower Ra value was achieved of combined feed rate and spindle speed optimization. The parameter Rz increased slightly for all optimizations in comparison with the conventional case, but the changes are insignificant. The parameter Rsm was increased where feed rate optimization was applied, but reduced when the spindle speed optimization as so as combined feed rate and spindle speed optimization were applied. It is evident that the combined feed rate and spindle speed optimization to maintain the constant cutting speed and constant feed per tooth is the option that produces the best results.

Table 4 Roughness measurement results

Roughness	Rz [µm]	Ra [µm]	Rsm [µm]
Conventional	2.28 ± 0.4	0.44 ± 0.07	60 ± 12
Feed rate opt.	2.6 ± 0.25	0.45 ± 0.07	64 ± 13
Spindle speed opt.	2.52 ± 0.21	0.42 ± 0.05	55 ± 12
Feed rate and spindle speed opt.	2.46 ± 0.36	0.40 ± 0.05	54 ± 13

Table 3 Machining test results

Tool life test	Conventional	Feed rate opt.	Spindle speed opt.	Feed rate and spindle speed opt.
Machining time per surface [min]	53	55	26	27.5
Number of surfaces machined per tool life [-]	8	8	23	25
Total machining time (per tool life) [min]	424	440	598	687.5
Total machined area (per tool life) [dm^2]	18.72	18.72	53.82	58.5

4.5 Power input of machine tool axes' measurement

The energy consumption of machine tool axes was measured using a CA8335 Qualistar Plus Three-Phase Power Analyzer to further compare the different milling strategies. Each measurement was made when milling one complete surface layer of the concave part. Only energy consumption of two machine tool axes was applicable because the main cutting movement is realized only in the X-Z plane and the *Y* axis is involved only during traversal movements. The characteristics of power input measured on the *X* and *Z* axes are seen in Fig. 20. The characteristics of power input for the case of milling with spindle speed optimization is not included in this figure, because they are practically the same as for the case of milling with feed rate and spindle speed optimization. The figure shows that the power input of the *X* axis is nearly the same for all cases of milling ((a) conventional, (b) feed rate optimization, (c) feed rate and spindle speed optimization). This means that the changing of the feed rate itself does not have a significant impact on energy consumption. The changes are seen on the characteristics of the *Z* axis, which is more loaded. This axis moves the headstock and spindle in a vertical direction. The case of conventional milling (Fig. 20a) shows that in the middle section of the characteristic (and also the middle toolpath section), the power input does not reach very variable values. In the case of milling with feed rate optimization, we can see that in the middle section of the characteristic, the power input reaches almost the same values, which means that the milling is smoothed. However, it is evident that at the initial section, the power input increased very little compared to the conventional case. In the last case, i.e. milling using both optimizations (feed rate and spindle speed), it is clear that the power input reaches almost the same values along the whole section of the toolpath, which means that the movements were smoothed.

5 Conclusion

A new method for feed rate optimization was proposed. This method is based on maintaining a constant feed per tooth for point milling toolpaths and relies on the integration of the angular velocity of the tool movement relative to the workpiece directly at the contact point between the tool and the workpiece. Using this feed rate optimization method, smooth movements are achieved directly at the contact point between the tool and the workpiece. It was verified that the control system can maintain the feed rate changes along the toolpath exactly as required by the optimization. The research showed that using this optimization method results in shorter production times for convex surfaces where feed

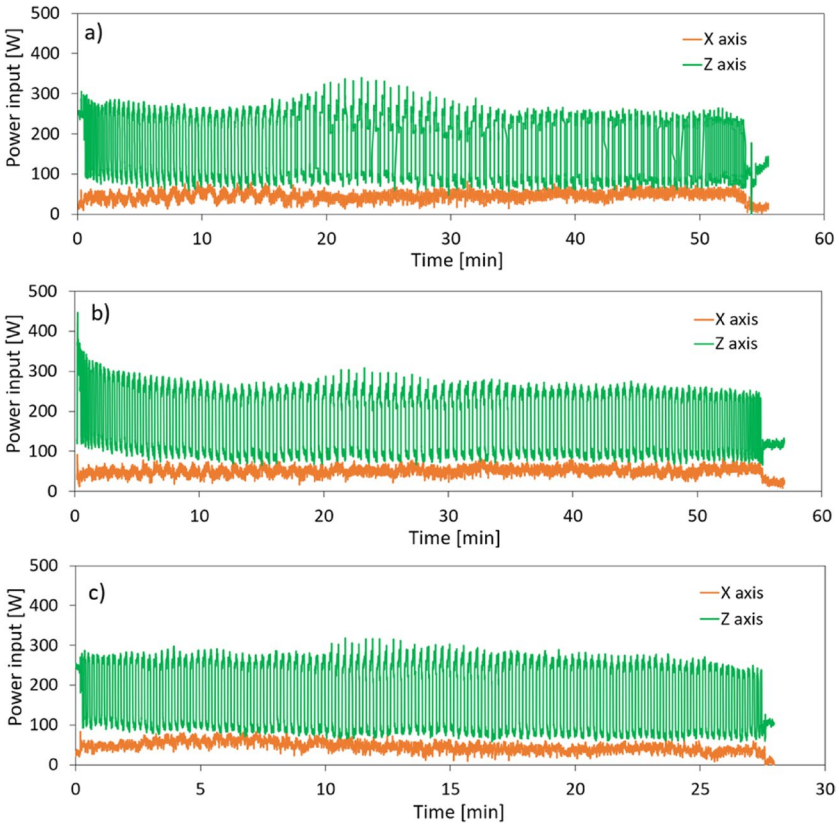

Fig. 20 The power input characteristics measured on the *X* and *Z* axes (**a** conventional, **b** feed rate optimization, **c** feed rate and spindle speed optimization)

rates are increased and conversely longer production times for concave surfaces where feed rates must be reduced to achieve a constant feed per tooth. It was also verified that feed rate control does not negatively affect the power input of the machine axes. In addition, by controlling the feed rate, practically uniform input power values were achieved compared to the conventional case. The highest benefits are achieved when the feed rate control method is combined with function for achieving the constant cutting speed, when the necessary technological conditions defined by the technologist during the toolpath creation in the CAM system are maintained. The best machined surface roughness and the best tool life were achieved with this optimization. The method can be implemented directly in a CAM system, and in this paper, the implementation was achieved through a post-processor, i.e., in the automatic generation of NC programs. It is necessary to add that no changes of toolpath are needed by using this optimization method. The method is verified for three-axis toolpaths. Although the method is also proposed for multi-axis toolpaths, it has not yet been validated in these cases. Validation for multi-axis toolpaths is assumed for further development in this topic.

Author contribution All authors contributed to the study conception and design. Material preparation, data collection, and analysis were performed by Petr Vavruska, Filip Bartos, and Matej Pesice. The first draft of the manuscript was written by Petr Vavruska and Filip Bartos. Review was carried out by Matej Pesice. Project administration was performed by Petr Vavruska. All authors read and approved the final manuscript.

Funding This publication was created based on the knowledge obtained within the project Machine Tools and Precision Engineering (MTPE), Reg. No. CZ.02.1.01/0.0/0.0/16_026/0008404. The knowledge was published in the publication "Automated feed rate optimization with consideration of angular velocity according to workpiece shape" which focuses on 2D toolpaths whereas this paper focuses on the solution for 3D toolpaths.

Declarations

Competing interests The authors declare no competing interests.

References

1. Gupta SK, Saini SK, Spranklin BW, Yao Z (2005) Geometric algorithms for computing cutter engagement functions in 2.5D milling operations. Comput-Aided Des 37:1469–1480. https://doi.org/10.1016/j.cad.2005.03.001
2. Uddin MS, Ibaraki S, Matsubara A, Nishida S, Kakino Y (2006) Constant engagement tool path generation to enhance machining accuracy in end milling. JSME Int J Ser C Mech Syst Mach Elem Manuf 49:43–49. https://doi.org/10.1299/jsmec.49.43
3. Ma J-W, Lu X, Li G-L, Qu Z-W, Qin F-Z (2020) Toolpath topology design based on vector field of tool feeding direction in sub-regional processing for complex curved surface. J Manuf Process 52:44–57. https://doi.org/10.1016/j.jmapro.2020.01.036
4. Bagri S, Manwar A, Varghese A, Mujumdar S, Joshi SS (2021) Tool wear and remaining useful life prediction in micro-milling along complex tool paths using neural networks. J Manuf Process 71:679–698. https://doi.org/10.1016/j.jmapro.2021.09.055
5. Mali RA, Gupta TVK, Ramkumar J (2021) A comprehensive review of free-form surface milling– advances over a decade. J Manuf Process 62:132–167. https://doi.org/10.1016/j.jmapro.2020.12.014
6. Ch L, Li Y, Jiang X, Shao W (2020) Five-axis flank milling tool path generation with curvature continuity and smooth cutting force for pockets. Chinese J Aeron 33:730. https://doi.org/10.1016/j.cja.2018.12.003
7. Ghorbani M, Movahhedi MR (2019) Extraction of surface curvatures from tool path data and prediction of cutting forces in the finish milling of sculptured surfaces. J Manuf Process 45:237–289. https://doi.org/10.1016/j.jmapro.2019.07.008
8. Zhang L, Zheng L (2005) Prediction of cutting forces in end milling of pockets. Int J Adv Manuf Technol 25:281–287. https://doi.org/10.1007/s00170-003-1841-5
9. Do TV, Phan TD (2021) Multi-objective optimization of surface roughness and MRR in milling of hardened SKD 11 steel under nanofluid MQL condition. Int J Mech Eng Robo Res 10:357–362. https://doi.org/10.18178/ijmerr.10.7.357-362
10. Wu B, Zhang Y, Liu G, Zhang Y (2021) Feedrate optimization method based on machining allowance optimization and constant power constraint. Int J Adv Manuf Technol 115:3345–3360. https://doi.org/10.1007/s00170-021-07381-z
11. Xie J, Zhao P, Hu P, Yin Y, Zhou H, Chen J, Yang J (2021) Multi-objective feed rate optimization of three-axis rough milling based on artificial neural network. Int J Adv Manuf Technol 114:1323–1339. https://doi.org/10.1007/s00170-021-06902-0
12. Liu D, Luo M, Pelayo GU, Trejo DO, Zhang D (2021) Position-oriented process monitoring in milling of thin-walled parts. J Manuf Syst 60:360–372. https://doi.org/10.1016/j.jmsy.2021.06.010
13. Park HS, Qi B, Dang DV, Park DY (2018) Development of smart machining system for optimizing feedrates to minimize machining time. J Comput Des Eng 5:299–304. https://doi.org/10.1016/j.jcde.2017.12.004
14. Hemmett JG, Fussell BK, Jerard RB (2000) Robust and efficient feedrate selection for 3-axis machining. IMECE Dyn Syst Cont 2:729–736. https://doi.org/10.1115/IMECE2000-2369
15. Ma JW, Song DN, Jia ZY, Hu GQ, Su WW, Si LK (2018) Toolpath planning with constraint of cutting force fluctuation for curved surface machining. Prec Eng 51:614–624. https://doi.org/10.1016/j.precisioneng.2017.11.002
16. Qin P, Wang M, Sun L (2020) Feed rate variation strategy for semi-conical shell workpiece in ball head end milling process. Appl Sci 10. https://doi.org/10.3390/app10249135
17. Sun G, Wright P (2014) Simulation-based cutting parameter selection for ball end milling. J Manuf Syst 24:352–365. https://doi.org/10.1016/S0278-6125(05)80019-6
18. Kiswanto G, Zariatin DL, Ko TJ (2014) The effect of spindle speed, feed-rate and machining time to the surface roughness and burr formation of Aluminum Alloy 1100 in micro-milling operation. J Manuf Process 16:435–450. https://doi.org/10.1016/j.jmapro.2014.05.003
19. Erkorkmaz K, Layegh SE, Lagozlu I, Erdim H (2013) Feedrate optimization for freeform milling considering constraints from the feed drive system and process mechanics. CIRP Annals 62:359–398. https://doi.org/10.1016/j.cirp.2013.03.084
20. García-Hernández C, Garde-Barace JJ, Valdivia-Sánchez JJ, Ubieto-Artur P, Bueno-Pérez JA, Cano-Álvarez B, Alcázar-Sánchez MÁ, Valdivia-Calvo F, Ponz-Cuenca R, Huertas-Talón JL, Kyratsis P (2021) Trochoidal milling path with variable

feed. Application to the Machining of a Ti-6Al-4 V Part. Mathematics 9(21):2701. https://doi.org/10.3390/math9212701
21. Vavruska P, Pesice M, Zeman P, Kozlok T (2022) Automated feed rate optimization with consideration of angular velocity according to workpiece shape. Results Eng 100762. https://doi.org/10.1016/j.rineng.2022.100762
22. Krajnik P, Kopač J (2004) Modern machining of die and mold tools. J Mat Proc Technol 157-158:543–552. https://doi.org/10.1016/j.jmatprotec.2004.07.146
23. Rahman AKMA, Feng HY (2013) Effective corner machining via a constant feed rate looping tool path. Int J Prod Res 51:1836–1851. https://doi.org/10.1080/00207543.2012.716170
24. Sodemann AA, Mayor JR (2011) Experimental evaluation of the variable-feedrate intelligent segmentation method for high-speed, high-precision micromilling. ASME. J Manuf Sci Eng 133:021001. https://doi.org/10.1115/1.4003010
25. Yau HT, Kuo MJ (2001) NURBS machining and feed rate adjustment for high-speed cutting of complex sculptured surfaces. Int J of Prod Res 39:21–41. https://doi.org/10.1080/00207540010002360
26. Mayor JR, Sodemann AA (2008) Intelligent tool-path segmentation for improved stability and reduced machining time in micromilling. ASME J Manuf Sci Eng 130:031121. https://doi.org/10.1115/1.2931492
27. Zhang Q, Li S, Guo J (2012) Smooth time-optimal tool trajectory generation for CNC manufacturing systems. J Manuf Syst 31:280–287. https://doi.org/10.1016/j.jmsy.2012.06.001
28. Chen M, Xi X-C, Zhao W-S, Chen H, Liu H-D (2017) A universal velocity limit curve generator considering abnormal tool path geometry for CNC machine tools. J Manuf Syst 44:295–301. https://doi.org/10.1016/j.jmsy.2017.04.010
29. Yeh SS, Hsu PL (2002) Adaptive-feedrate interpolation for parametric curves with a confined chord error. Comp-Aid Des 34:229–237. https://doi.org/10.1016/S0010-4485(01)00082-3
30. Farouki RT, Manjunathaiah J, Nicholas D, Yuan GF, Jee S (1998) Variable-feedrate CNC interpolators for constant material removal rates along Pythagorean-hodograph curves. Comput-Aided Des 30:631–640. https://doi.org/10.1016/S0010-4485(98)00020-7
31. Tikhon M, Ko TJ, Lee SH, Sool Kim H (2004) NURBS interpolator for constant material removal rate in open NC machine tools. Int J Mach Tools Manuf 44:237–245. https://doi.org/10.1016/j.ijmachtools.2003.10.020
32. Farouki RT, Tsai YF (2001) Exact Taylor series coefficients for variable-feedrate CNC curve interpolators. Comput-Aided Des 33:155–165. https://doi.org/10.1016/S0010-4485(00)00085-3
33. Tsai YF, Farouki RT, Feldman B (2001) Performance analysis of CNC interpolators for time-dependent feedrates along PH curves. Comput Aided Geom Des 18:245–265. https://doi.org/10.1016/S0167-8396(01)00029-2
34. Zhang D-L, Zhou L-S (2009) Adaptation of feed rate for 3-axis CNC high-speed machining. J Harbin Inst Technol 16:391–395
35. Sencer B, Ishizaki K, Shamoto E (2015) A curvature optimal sharp corner smoothing algorithm for high-speed feed motion generation of NC systems along linear tool paths. Int J Adv Manuf Technol 76:1977–1992. https://doi.org/10.1007/s00170-014-6386-2
36. Ward R, Sun C, Dominguez-Caballero J, Ojo S, Ayvar-Soberanis S, Curtis D, Ozturk E (2021) Machining Digital Twin using real-time model-based simulations and lookahead function for closed loop machining control. Int J Adv Manuf Technol 117:3615–3629. https://doi.org/10.1007/s00170-021-07867-w
37. Vavruska P, Zeman P, Stejskal M (2018) Reducing machining time by pre-process control of spindle speed and feed-rate in milling strategies. Procedia CIRP 77:578–581. https://doi.org/10.1016/j.procir.2018.08.216
38. Käsemodel RB, de Souza AF, Voigt R, Basso I, Rodrigues AR (2020) CAD/CAM interfaced algorithm reduces cutting force, roughness, and machining time in free-form milling. Int J Adv Manuf Technol 107:1883–1900. https://doi.org/10.1007/s00170-020-05143-x
39. Vavruska P, Bartos F, Stejskal M, Pesice M, Zeman P, Heinrich P (2023) Increasing tool life and machining performance by dynamic spindle speed control along toolpaths for milling complex shape parts. J Manuf Process 99:283–297. https://doi.org/10.1016/j.jmapro.2023.04.058
40. Segonds S, Seitier P, Bordreuil C, Bugarin F, Rubio W, Redonnet JM (2019) An analytical model taking feed rate effect into consideration for scallop height calculation in milling with torus-end cutter. J Intell Manuf 30:1881–1893. https://doi.org/10.1007/s10845-017-1360-0